Portable Wide-Angle γ-Ray Vision Systems

Z. He, S.V. Guru, D.K. Wehe, G.F. Knoll
Department of Nuclear Engineering,
The University of Michigan, Ann Arbor, MI 48109.

A. Truman, D. Ramsden
Physics Department, Southampton University,
Southampton, U.K. SO17 1BJ.

Abstract

The characteristics of two portable γ-ray vision systems, which could be transported by a robot, have been explored and compared. The detector of the first system (CSPMT) consists of an array of 37 CsI(Na) scintillation crystals viewed by a single 5 inch diameter position-sensitive photomultiplier tube (PSPMT), while the second system (CSPD) employs an array of 40 CsI(Tl) scintillation detectors coupled to PIN silicon photodiodes. These devices are designed to operate in the energy range from 70 keV to 1.5 MeV, which encompasses most energies of γ-ray radiation from the radioactive nuclides of interest to the nuclear industry.

These systems have good angular resolutions of about 3° FWHM at the central field of view of 10°×10° or better when image reconstruction is employed, and coarser angular resolutions of about 10° FWHM elsewhere within a wide field of view of 50°×50°. The energy resolution of both systems have been tested using individual detector elements, and the imaging performance of proposed full systems have been simulated using a prototype. Our results show that these devices should be good candidates for the next generation portable γ-ray imaging systems.

I. Introduction

Portable γ-ray imaging detectors for the energy range from 70 keV to 1.5 MeV are required for a large number of applications in the nuclear industry, such as radiation monitoring in nuclear power plants, radioactivity distribution measurements for nuclear waste inspections, and radiation detection in contaminated rooms or post accident conditions. In some applications, the instrument would be carried on a robot.

In order to observe γ-ray spatial distributions, many imaging techniques have been developed. Coded-mask detectors using Uniformly-Redundant Arrays [1, 2, 3, 4] and Rotation-Modulation Collimators [5, 6] have been extensively employed in γ-ray astronomy due to their high transparency, which is important for obtaining maximum detection efficiency. Their performance is superior to conventional collimators for point sources, but deteriorates severely for extended sources. Compton-scatter γ-ray imagers have also been used in astronomical observations [7] and have been investigated for radiation monitoring [8]. Good performance of this type of instrument has been demonstrated, but the large physical dimensions limit their portability.

The use of diverging multi-hole collimators [9, 10] and pinhole collimators [11] have been practical choices to observe distributed sources. A pinhole collimator is easy to fabricate and operate, but has practical limitations, such as the minimum diameter of the hole has to be comparable to the thickness of the shield, the trade-off between the spatial resolution and the field of view for a limited detector area, the weight restrictions and the position resolution of the detector. It is difficult to obtain a spatial resolution better than about 5° on a portable pinhole camera in the energy range of our interest. Although a multi-hole collimator is harder to fabricate, it does have some advantages. For example, it has better stopping power for γ-rays than a pinhole collimator since it can be constructed using a thicker shield. Moreover, the field of view of a γ-ray imager using a multi-hole collimator can be much wider than that using a pinhole collimator since its detection efficiency for an object moving from the center to the edge of the field of view does not drop significantly. In contrast, there is a severe decrease in efficiency for a pinhole collimator.

Two generations of γ-ray imaging systems have been constructed and tested at the University of Michigan. The first system was a single-shutter camera [12] which used a lead-shielded BGO scintillator coupled to a photomultiplier tube. The second system [13] employs a diverging multi-hole collimator and a 7.5×7.5×1 cm NaI(Tl) detector viewed by a 3 inch square position-sensitive photomultiplier tube. The proposed wide-angle portable vision systems described in this paper employ multi-hole collimators, but have new arrangements in the hole patterns in order to make efficient use of limited number of holes,

*This work was supported under the U.S. Department of Energy, Robotics for Hazardous Environments, Grant No. DOE-FG02-86NE37969.

0018-9499/95$4.00

and have a 180° rotation anti-symmetric structure which will greatly enhance the quality of the observed image, especially when the background from the penetration of γ-rays through the shield becomes unacceptable for a conventional multi-hole collimator. Furthermore, the detectors of these instruments consist of discrete CsI scintillation crystals with a length of 3 cm, which is necessary to obtain a good detection efficiency for γ-rays above 1 MeV. A prototype has been built and the imaging performance of the proposed systems has been investigated using the experimental results of the prototype.

II. Two Proposed Systems

The designs for the two imaging cameras are shown in Figures 1 and 2. The CSPMT system consists of an array of 37 CsI(Na) scintillation crystals viewed by a single 5 inch diameter position-sensitive photomultiplier tube (PSPMT). The choice of sodium doped CsI crystals is due to their higher scintillation conversion efficiency compared with thallium doped CsI, although CsI(Na) has to be sealed due to its hygroscopic characteristic. The CSPD system employs an array of 40 CsI(Tl) scintillation detectors coupled to PIN silicon photodiodes. This configuration is more compact and makes use of the detection volume of the scintillators more efficiently. Both devices are designed to operate in the energy range from 70 keV to 1.5 MeV, which is of principal interest to the nuclear industry.

Both devices employ diverging multi-hole collimators as shown in Figures 1 and 2. In order to make efficient use of the limited number of holes, the collimators are designed to provide a good angular resolution of 3°×3° FWHM within the central field of view of about 10°×10°, and a coarser angular resolution of about 10° FWHM elsewhere in a wide field of view of 50°×50°. The radiation distribution of an area of special interest can be studied by pointing the camera at that area, while objects within a wide field of view are also observed with a lower resolution. Moreover, the patterns of both collimator apertures are designed to be 180° anti-symmetric relative to the axis of rotation at the center of the devices. Figure 3 illustrates the collimator pattern of the CSPD system as an example. Source and background observations can be made simply by rotating the collimator 180° around the central axis. This design will minimize most of the systematic errors in estimating the source flux, such as those caused by septal and shield penetration of γ-rays.

Each 4 mm ϕ aperture of the collimator of the CSPMT system is observed by a 1.5×1.5×3 cm CsI(Na) crystal, and 37 of these detector elements are viewed by a single 5 inch diameter PSPMT. The width of each CsI(Na) crystal has to be larger than the lateral displacement of incident γ-rays at the bottom of the detector in order to minimize the interference between different detector elements. The cross-section of apertures of the CSPD system is 6 mm

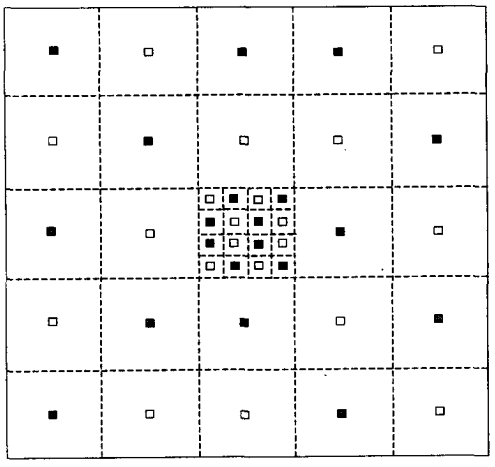

Figure 3: Pointing Directions of Corresponding Apertures within the Field of View of the CSPD System.

square. Each of these apertures is observed by a 1×1×3 cm CsI(Tl) scintillation crystal coupled to a 1 cm^2 PIN silicon photodiode. These crystals are aligned along the pointing directions of corresponding apertures so that the stopping power of these detectors can be fully used. The choice of scintillator size is more flexible in the CSPD configuration. The dimension of 1×1×3 cm was chosen since both good detection efficiency and energy resolution can be obtained at this size using currently available technology. The sides and rear of both systems are shielded by 3 cm thick tungsten. The weight of both systems is estimated to be less than 70 kilograms.

When these devices are carried on robots during observations, the pointing direction of the instrument would be controlled by the robotic system, otherwise, a pan-and-tilt table will be required.

III. Energy Resolutions

The energy resolution of the CSPMT system has been tested by using two 1.5×1.5×3 cm CsI(Na) crystals on one 5 inch diameter PSPMT. The crystals were made at the BICRON Newbury plant. Energy resolutions of about 7% FWHM at 662 keV were obtained. Previous experience with PSPMTs [14, 15] has shown that there should be no difficulty in recognizing the detector element in which γ-rays deposit their energy, and in distinguishing between single-bar events and multi-bar scattering. This has also been confirmed by experimental tests using the two CsI(Na) crystals. The ability to distinguish between single and multi-bar events will help to minimize the interference between different detector elements and to increase the photopeak ratio since each detector element can be actively shielded by the surrounding scintillators.

The energy resolution of CSPD system has also been tested using a REXON 1×1×3 cm CsI(Tl) crystal cou-

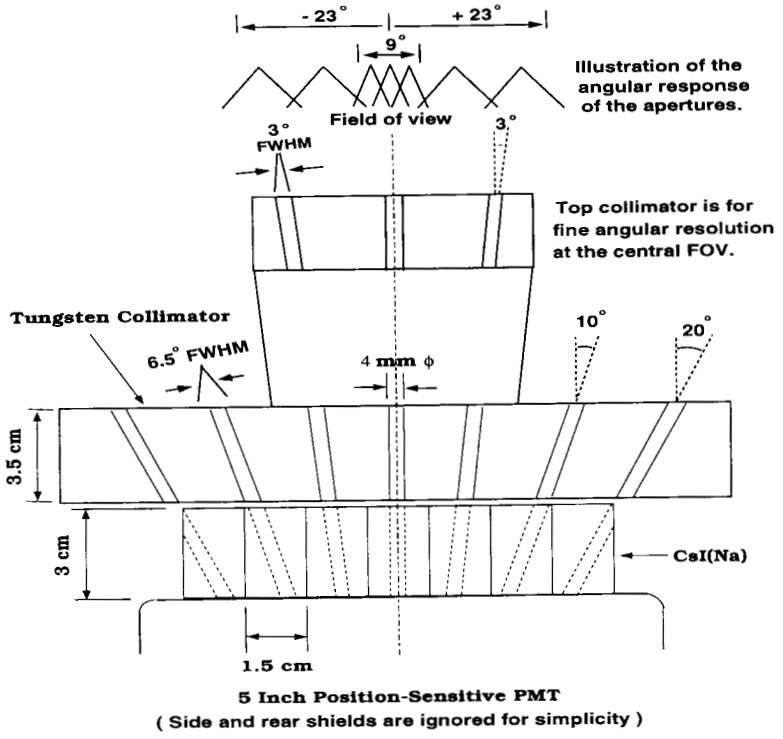

Figure 1: Section View of the CSPMT system.

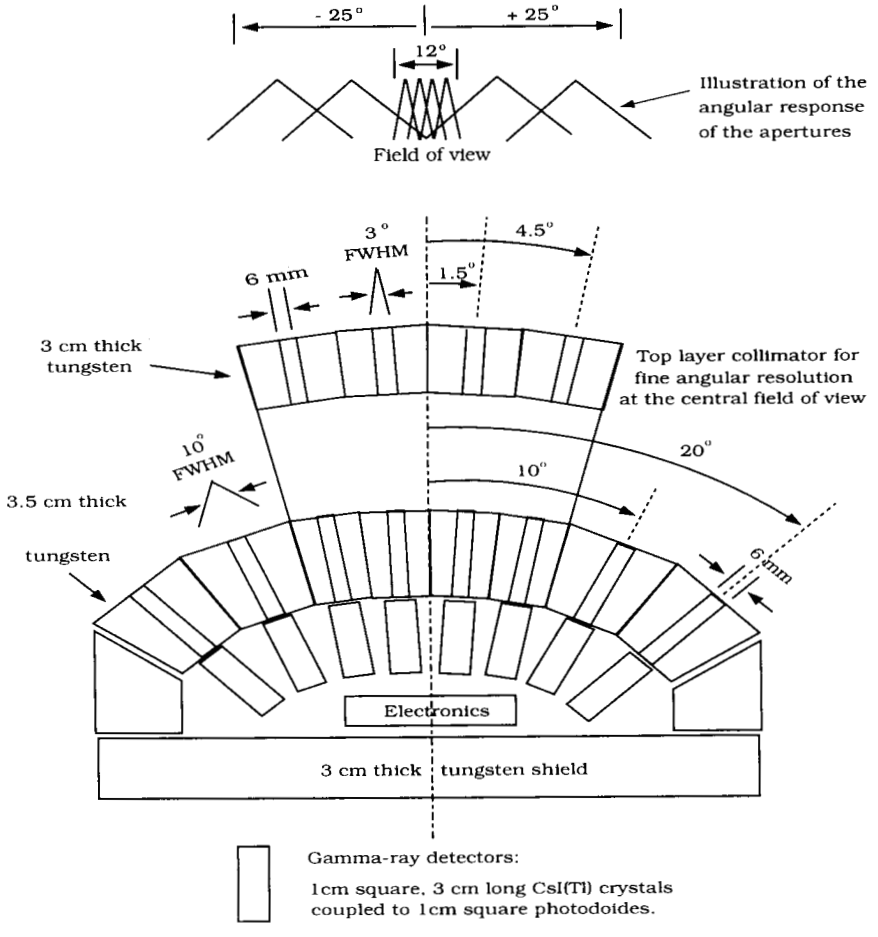

Figure 2: Section View of the CSPD System.

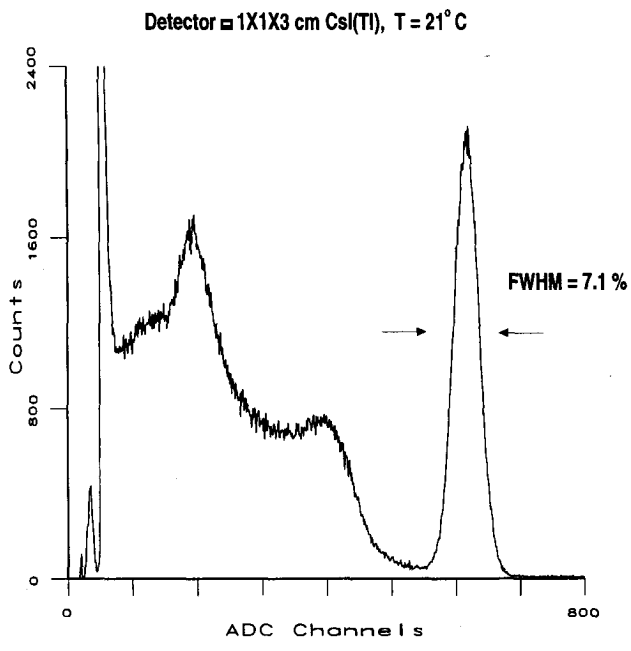

Figure 4: Energy Spectrum of the CSPD System at 662 keV.

pled to a 1 cm^2 Hamamatsu S3590-03 photodiode. An AMPTEK A250 charge-sensitive preamplifier and an ORTEC 572 shaping amplifier were used. Due to the good quality of the crystal, an energy resolution of 7.1% FWHM at 662 keV was obtained as shown in Figure 4.

Comparing the two systems, the CsI(Na)/PSPMT detectors have better performance below about 600 keV, while the CsI(Tl)/Photodiode detector has superior energy resolution at higher energies.

IV. Modeling Results

The detection efficiencies of the detectors and the performance of the shields have been simulated using GEANT3 [16]. The results of Monte-Carlo simulations show that the 3.5 cm thick tungsten collimators will stop 90% of normally incident 1333 keV γ-rays of ^{60}Co. The sensitivities of both systems have been estimated based on the full-energy detection efficiencies obtained using Monte-Carlo simulations and background measurements using individual detector elements in our laboratory. The results show that the CSPMT system should be able to detect a 2 mCi ^{137}Cs source located 5 meters from the detector with 3 σ detection significance in about 1 minute, while the CSPD system can detect a 0.5 mCi source during the same period. These predictions have been confirmed by our experimental results shown in the next section.

V. Results from the Prototype

A. *Prototype Configurations*

In order to investigate the imaging performance of the proposed systems and to test their sensitivities, a prototype system was built and has been tested. A picture of this prototype is shown in Figure 5. For economy, its collimator is made of two layers of lead disks having 1 inch thickness due to the ready availability of the material. The inner collimator disk can be rotated along its axis and is accurately controlled by a stepping motor. Both layers of the collimator have one 6 mm square aperture. Since both apertures are located 2 cm from the centers of the disks, the signal and background observations can be carried out by aligning the two apertures and rotating the aperture on the inner layer collimator to the opposite side. The separation between the two layers of collimators can be continuously adjusted to vary the field of view. The detector used was the 1×1×3 cm CsI(Tl) crystal coupled to a 1 cm square photodiode. An AMPTEK A250 charge-sensitive preamplifier was used with an ORTEC 572 shaping amplifier. The detector was shielded by 1 inch thick lead around four sides, and the bottom was left open for the convenience of changing detectors. The collimator and the detector were mounted on a pan-and-tilt table which can be rotated in two dimensions controlled by a 486 PC. By pointing the detector in different directions, the imaging performance of the detector arrays proposed for the full systems can be simulated. The block diagram of the prototype system is shown in Figure 6.

B. *Spatial Resolution*

The spatial resolution at 662 keV within the central field of view of the proposed systems has been tested by setting the geometric FWHM of the field of view of the aperture on the prototype to be 3°. This should be the spatial resolution at lower γ-ray energies since the septal penetration length is small compared with the thickness of the collimator. A 10 mCi ^{137}Cs source was located at 1 meter from the collimator. The pointing direction of the prototype scanned at 0.5° steps across a 14°×14° field of view centered at the source. The observation time at each direction was 1 minute. The counts under the 662 keV photopeak as a function of pointing direction of the prototype is shown in Figure 7. The data shows that the actual FWHM of the field of view of the aperture is about 4° at 662 keV, while the geometric FWHM of the aperture was set to be 3°. The spatial resolution will become worse for γ-rays at even higher energies.

C. *Sensitivity*

The sensitivity of a γ-ray detector is a function of incident γ-ray energy and background radiation. We have investigated the sensitivity of the proposed systems in laboratory environment (weak background) in order to compare with

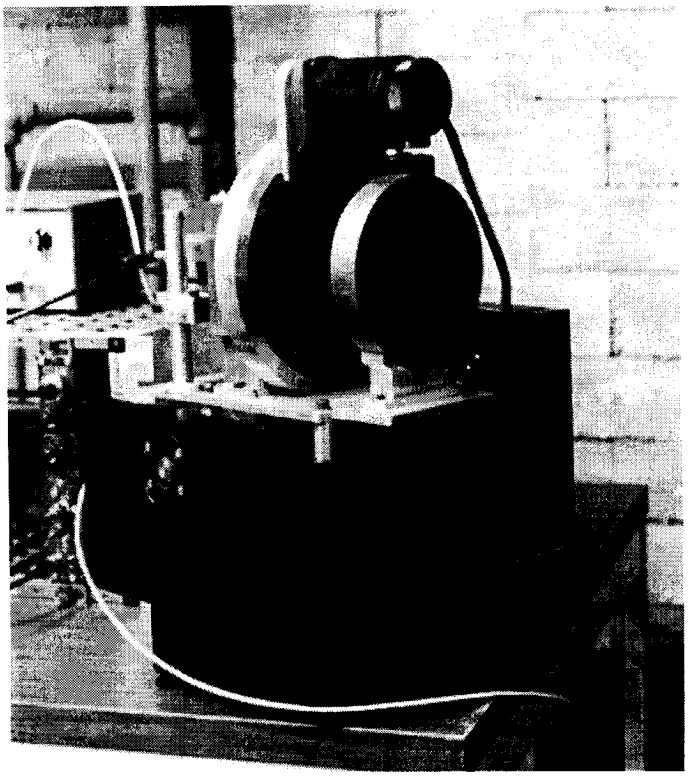

Figure 5: The Prototype System.

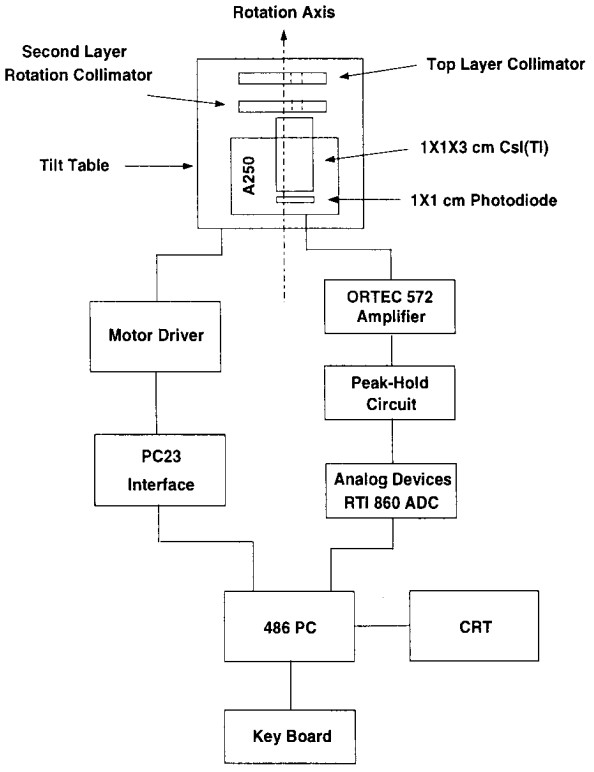

Figure 6: Block Diagram of the Prototype System.

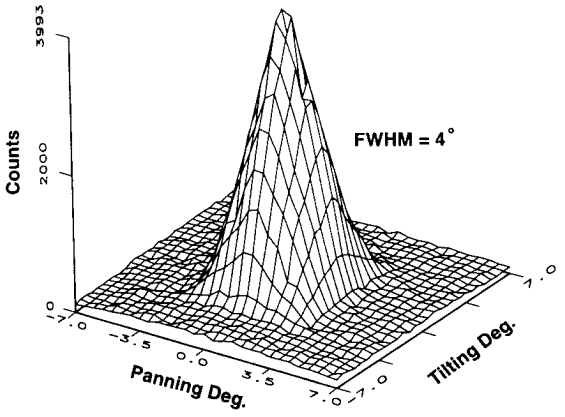

Figure 7: Point Response Function (1 meter) at 662 keV.

our Monte-Carlo simulations. A 10 μCi ^{137}Cs source was located at a distance of 1 meter from the collimator of the prototype. We scanned the pointing direction of the device in 1.5° steps in both panning and tilting directions within a field of view of 12°×12° centered on the source direction. This experiment simulated what we would obtain from the central 3×3 detector elements of the CSPMT system after we scan a 3×3 directional array, or similar to what we could get from the central 4×4 detectors of the CSPD system after scanning 2×2 directions with equal steps of 1.5°. The observation time at each pointing direction was 1 hour. A signal to noise ratio of about 12 was obtained at the source direction and the results can be seen in Figure 8. It can be shown that these results are consistent with predictions of sensitivities using Monte-Carlo simulations, which showed that the CSPD system should be able to detect a 0.5 mCi ^{137}Cs source located 5 meters from the detector with 3 σ detection significance in about 1 minute. It should be noted that this sensitivity measurement provides a conservative estimation since only 1 inch thick lead was used to shield the detector instead of proposed thicker tungsten shielding, and the bottom of the detector was not even shielded.

D. *Image Reconstruction*

In order to avoid dead areas within the field of view, the pointing directions of apertures of the proposed systems are arranged in a way that when a remote point source moves within the central field of view of the systems, the effective detection area is kept constant. This can be seen in Figures 1 and 2. On the other hand, the incident γ-rays from a point source will be detected by up to four apertures pointing around the direction of the source unless it happens to be located exactly on the axis of one aper-

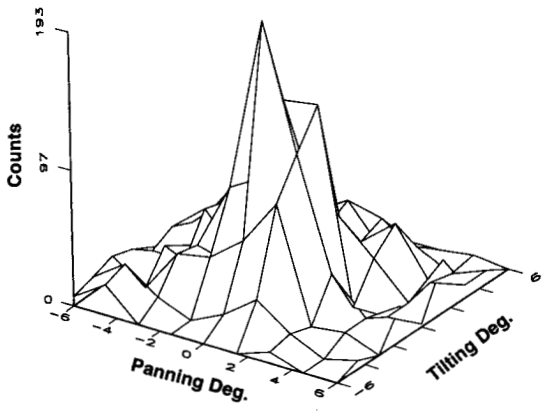

Figure 8: Observations of 9×9 Directions After Background Subtraction.

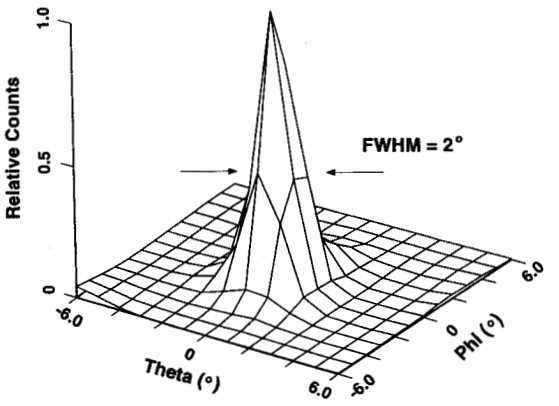

Figure 9: Source Distribution After Image Reconstruction (MLEM).

ture. This means that the observed image is a 'smeared' source distribution, i.e., the convolution of the true source distribution and the point response function of the system.

The true source distribution may be estimated using an image reconstruction method that includes the knowledge of the response of the system as a function of incident γ-ray direction. This has been tested using the raw observational data shown in Figure 8 and the point response function shown in Figure 7. An algorithm based on the Maximum-Likelihood Expectation Maximization (MLEM) method [17] was used and about 2° FWHM of the source distribution was obtained. The results are shown in Figure 9. It is evident that the image quality can be greatly enhanced through the image reconstruction process. In another test, we scanned the pointing direction at finer steps of 1° within a field of view of 12°×12° centered at a 10 mCi ^{137}Cs point source located 1 meter from the collimator. One minute was the observation time at each direction. The observed signal to noise ratio was very high due to the intense activity of the source. A FWHM of about 1° was obtained on the source distribution.

VI. Conclusions

The moderate sensitivity of being able to detect a few milli-Curie source from 5 meters away within 1 minute, wide field of view of about 50°×50°, good spatial resolution of about 3° FWHM or better when image reconstruction is employed, and compactness of the devices make these instruments good candidates for next generation portable γ-ray vision systems. The CSPMT system has simpler readout electronics, better energy resolution below about 600 keV and lower cost. The CSPD system offers better energy resolution at higher energies, better sensitivity, wider field of view and it is more robust.

Acknowledgments

We would like to thank Dr. G.J. Daniell of Southampton University for providing his Maximum-Entropy program for our data processing, as well as Prof. J. Lee of the University of Michigan for his help in our imaging reconstruction. We are also very grateful to Prof. Tipei Li of IHEP of Beijing and Dr. S.N. Zhang of NASA MSFC for their valuable discussions.

References

[1] E.E. Fenimore & T.M. Cannon, "Coded aperture imaging with uniformly redundant arrays", *Applied Optics*, vol. 17(3), pp. 337–347, 1978.

[2] W.R. Cook et al., "Gamma-ray imaging with a rotation hexagonal uniformly redundant array", *IEEE Transactions on Nuclear Science*, vol. 31(1), pp. 771–775, 1984.

[3] J.E. Grindlay et al., "The energetic x-ray imaging telescope experiment (exite)", *IEEE Transactions on Nuclear Science*, vol. 33(1), pp. 750–754, 1986.

[4] "INTEGRAL, report on the phase a study, ESA SCI(93)1", 1993.

[5] L. Mertz, "A dilute image transform with application to an x-ray star camera", *Morden Optics*, vol. , pp. 787–791, 1967.

[6] A.M. Cruise, "Aperture synthesis in x-ray astronomy", *Mon. Not. R. astr. Soc.*, vol. 170, pp. 305–312, 1975.

[7] P.von Ballmoos et al., "Imaging the gamma-ray sky with compton telescope", *Astronomy and Astrophysics*, vol. 221, pp. 396–406, 1989.

[8] J.B. Martin et al., "Imaging multi-energy γ-ray fields with a compton scatter camera", *IEEE Transactions on Nuclear Science*, vol. 41, pp. 1019–1025, 1994.

[9] S.V. Guru et al., "Monte Carlo modelling of a multiple-hole collimator for high energy gamma-ray imaging", *IEEE Transactions on Nuclear Science*, vol. 41, pp. 898–902, 1994.

[10] R.H. Redus et al., "A nuclear survey instrument with imaging capability", *IEEE Transactions on Nuclear Science*, vol. 33, pp. 1354–1357, 1992.

[11] R.H. Redus et al., "A combined video and gamma ray imaging system for robots in nuclear environments", accepted for publication in *Nuclear Instruments and Methods.*

[12] T.A. DeVol et al., "Gamma-ray spectral imaging using a single-shutter radiation camera", *Nuclear Instruments and Methods*, vol. A299, pp. 495–500, 1990.

[13] S.V. Guru et al., "A portable gamma camera for radiation monitoring", *Conference Record of 1994 IEEE Nuclear Science Symposium and Medical Imaging Conference, Norfolk, Virginia. Oct.30 - Nov.5, 1994.*

[14] Z. He & D. Ramsden, "A broad-band position sensitive phoswich detector for γ-ray astronomy", *Nuclear Instruments and Methods*, vol. A336, pp. 330–335, 1993.

[15] C.J. Hailey et al., "An inexpensive, hard x-ray imaging spectrometer for use in x-ray astronomy and atomic physics", *Nuclear Instruments and Methods*, vol. A276, pp. 340–346, 1989.

[16] "GEANT detector description and simulation tool", CERN Program library long writeup W5013, June 1993.

[17] K. Lange & R. Carson, "EM reconstruction algorithms for emission and transmission tomography", *Journal of Computer Assisted Tomography*, vol. 8(2), pp. 306–316, 1984.